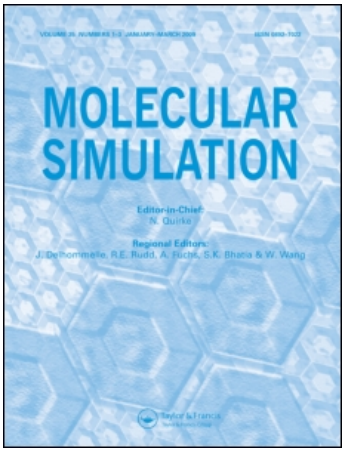

Molecular Simulation
Publication details, including instructions for authors and subscription information:
http://www.informaworld.com/smpp/title~content=t713644482

Structure, energetics and properties of some molecules with potent anti-HIV activity: a theoretical study

Debduti De[a]; Sudipta Dalai[a]; Bhudeb De[a]
[a] Department of Chemistry and Chemical Technology, Vidyasagar University, Midnapore, 721102, India

Online publication date: 11 May 2010

To cite this Article De, Debduti , Dalai, Sudipta and De, Bhudeb(2010) 'Structure, energetics and properties of some molecules with potent anti-HIV activity: a theoretical study', Molecular Simulation, 36: 6, 434 — 447
To link to this Article: DOI: 10.1080/17458080903583931
URL: http://dx.doi.org/10.1080/17458080903583931

Molecular Simulation
Vol. 36, No. 6, May 2010, 434–447

Taylor & Francis
Taylor & Francis Group

Structure, energetics and properties of some molecules with potent anti-HIV activity: a theoretical study

Debduti De, Sudipta Dalai and Bhudeb De*

Department of Chemistry and Chemical Technology, Vidyasagar University, Midnapore 721102, India

(*Received 15 August 2009; final version received 28 December 2009*)

Density functional theory (DFT; B3LYP) and Hartree–Fock (HF; 3-21G, 6-31G(d) and 6-311G(d,p)) calculations with complete geometry optimisations are carried out in the ground state on five 6-aminoquinolone derivatives, which have been proved to be highly effective in inhibiting HIV replication, to study their structures, energetics and HOMO–LUMO correlation with physiological action. The gas-phase calculations and single-point polarisable continuum model water-phase calculations show that the molecules are highly effective in inhibiting HIV replication, which is in excellent agreement with the experiment. Structural features, energies, charge densities and HOMO–LUMO correlation have been found to substantiate the experimental findings. Compound **4** (pyrazine) shows some special features in DFT calculations which are not found in HF calculations. In the present series, HF results are more reliable as expected.

Keywords: Gaussian; density functional theory (B3LYP); Hartree–Fock; gas phase; potent molecules

1. Introduction

Discovery of compounds with highly active anti-retroviral therapy is still a challenging task for new anti-HIV agents. Quinolones have been pursued as new potential candidates for the treatment of AIDS [1–6]. Recently, a series of 6-aminoquinolones variously substituted in the different position of the quinolone nucleus [6] have been prepared [7]. Among them, **1** was the lead compound and the structural modification around it permitted to obtain new potent anti-HIV-1 and anti-HIV-2, 6-aminoquinolones **2**, **3**, **4** and **5**.

The purpose of the present work is to investigate theoretically the structure and properties in the ground state of the said compounds by Hartree–Fock (HF) and density functional theory (DFT; B3LYP) with 3-21G, 6-31G(d) and 6-311G(d,p) calculations [8–10] and to correlate the properties with physiological action (i.e. target specificity, transport ability and drug action), including the basis set effect. For an analysis of drug action, a solvent-phase calculation using water was carried out for these molecules.

2. Computational details

Complete geometry optimisations for all the molecules were done in the ground state by the HF and DFT (B3LYP) methods with 3-21G, 6-31G(d) and 6-311G(d,p) basis sets using the Gaussian 03W program [8–10]. The optimisation in the solvent phase could not be done because of very long computation time. Since HF results are systematic in the present series, the single-point water-phase calculations by the polarisable continuum model (PCM) have been carried out to have a first-hand information in the solution phase by the HF method using only the 6-311G(d,p) set at the gas-phase equilibrium geometry.

3. Results and discussion

Equilibrium geometries in the gas phase of the studied molecules by the DFT and HF methods are shown in Figures 1(a)–(e) and 2(a)–(e), respectively, with the numbering schemes in the 6-311G(d,p) basis set. The molecules are listed in Tables 1 and 2, along with their abbreviated names and computed total energies (hartree), dipole moments (debye), HOMO–LUMO energies (hartree) and ΔE-gap (hartree) between them by the DFT and HF (including the water-phase) methods, respectively. Tables 3 and 4 summarise the computed net Mulliken charge by the DFT and HF (along with the water-phase result) methods on the heteroatoms of the molecules in their respective optimised ground state. Atomic charge is not an observable quantum mechanical property. All methods for computing the atomic charges are necessarily arbitrary. Electron density among the atoms in a molecular system is being partitioned. The Mulliken population analysis computes charges by dividing orbital overlap equally between the two atoms involved. The values also depend on the basis set used. Therefore, the values are non-unique. Still, it is widely used to have an idea of electron

*Corresponding author. Email: brdranjan@yahoo.com

ISSN 0892-7022 print/ISSN 1029-0435 online

DOI: 10.1080/17458080903583931
http://www.informaworld.com

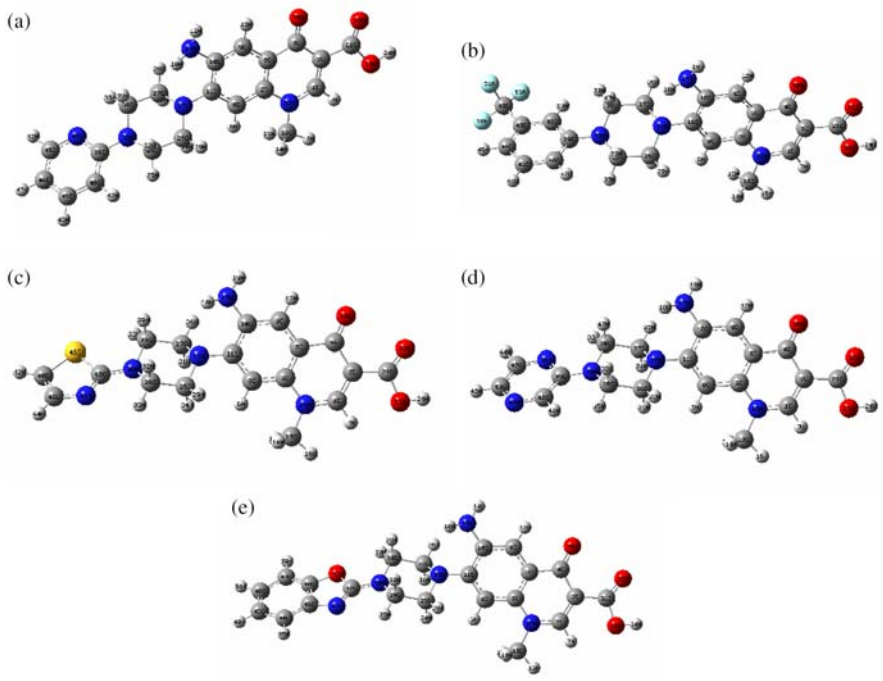

Figure 1. (a)–(e) Optimised structures of the five molecules (**1**–**5**), respectively, by the DFT (B3LYP) method (6-311G(d,p)).

density distribution in a molecular system. From Tables 1 and 2, it can be seen that in the gas phase, all the molecules are highly stable in the equilibrium ground state, the stability being the highest in the 6-311G(d,p) calculations. This indicates that they will also be more stable in the solution phase (verified by the single-point water-phase calculation) since each molecule has a hydrophilic part (4-keto-3-carboxylic moiety) and will also possess potent anti-HIV activity, which is in excellent agreement with the experimental results [7]. The first-hand information obtained from the single-point water-phase calculations by the HF method indicates more stability in the water phase than the gas phase for all the molecules. The dipole moment values reflect the overall charge distribution in a molecular system. The dipole moments (calculated by the DFT method) of **1** (lead compound), **3** (thiazole) and **4**

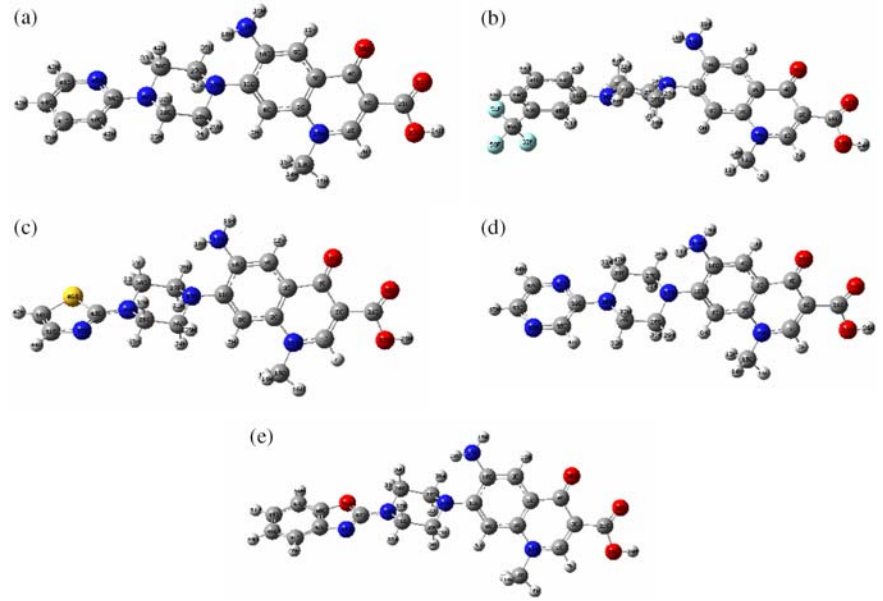

Figure 2. (a)–(e) Optimised structures of the five molecules (**1**–**5**), respectively, by the HF method (6-311G(d,p)).

Table 1. Computed total energies (hartree), dipole moments (debye), HOMO, LUMO energies (hartree) and ΔE(HOMO–LUMO gap) (hartree) at the equilibrium geometry of the ground state of the five molecules by the DFT (B3LYP) method.

Properties	Basis set	**1** (Lead compound)	**2** (Trifluoro)	**3** (Thiazole)	**4** (Pyrazine)	**5** (Benzoxazole)
Total energy	3-21	− 1267.22	− 1586.48	− 1586.43	− 1283.15	-1417.82
	6-31G(d)	− 1274.22	− 1595.21	− 1594.98	− 1290.25	− 1425.66
	6-311G(d,p)	− 1274.55	− 1595.64	− 1595.31	− 1290.58	− 1426.03
Total dipole moments	3-21	8.85	7.24	6.55	6.31	5.94
	6-31G(d)	9.17	7.64	7.02	6.79	6.27
	6-311G(d,p)	9.21	7.59	7.03	6.84	6.21
HOMO	3-21	− 0.1858	− 0.1906	− 0.1905	− 0.1893	− 0.1909
	6-31G(d)	− 0.1963	− 0.1999	− 0.1998	− 0.1994	− 0.2008
	6-311G(d,p)	− 0.2044	− 0.2085	− 0.2079	− 0.2075	− 0.2091
LUMO	3-21	− 0.0331	− 0.0369	− 0.0366	− 0.0368	− 0.0370
	6-31G(d)	− 0.0395	− 0.0425	− 0.0422	− 0.0428	− 0.0432
	6-311G(d,p)	− 0.0489	− 0.0523	− 0.0516	− 0.0521	− 0.0527
ΔE	3-21	0.1527	0.1537	0.1539	0.1525	0.1539
	6-31G(d)	0.1568	0.1574	0.1576	0.1566	0.1576
	6-311G(d,p)	0.1555	0.1562	0.1563	0.1554	0.1564

(pyrazine) are the highest in the 6-311G(d,p) calculations. The same for **2** (trifluoro) and **5** (benzoxazole) are the highest in the 6-31G(d) calculations. The HF results are more reliable in this respect. The dependence on the basis set is much less in the HF calculations.

From Table 1, it can also be seen that the HOMO and LUMO energies are in the order 3-21 < 6-31G(d) < 6-311G(d,p) as expected by the DFT method, but in Table 2, the same trend is followed for the HOMO energies, whereas the LUMO energies do not follow the same order by the HF calculations. The interesting point is that the ΔE-gap is almost identical for all the molecules and in all the basis sets by both the methods (with the exception of HF 6-31G(d), where it is slightly higher), showing that their activity towards chemical attack is also equivalent. However, the values calculated by the HF method are 2.5 times greater.

From Table 3, it can also be seen that the charge densities calculated by the 6-311G(d,p) basis set are systematically lower than the values obtained by the other two basis sets by both the methods (with some minor exceptions). It can also be seen that the charge densities obtained by the 6-31G(d) basis set are reasonable by both the methods for all the potent molecules.

Table 2. Computed total energies (hartree), dipole moments (debye), HOMO, LUMO energies (hartree) and ΔE(HOMO–LUMO gap) (hartree) at the equilibrium geometry of the ground state of the five molecules by the HF method.

Properties	Basis set	**1** (Lead compound)	**2** (Trifluoro)	**3** (Thiazole)	**4** (Pyrazine)	**5** (Benzoxazole)
Total energy	3-21	− 1259.39	− 1577.30	− 1578.45	− 1275.27	− 1409.15
	6-31G(d)	− 1266.44	− 1586.06	− 1587.04	− 1282.43	− 1417.06
	6-311G(d,p)	− 1266.74	− 1586.44	− 1587.34	− 1282.73	− 1417.38
	6-311G(d,p) (water phase)	− 1266.78	− 1586.49	− 1587.39	− 1282.77	− 1417.43
Total dipole moments	3-21	9.97	7.81	7.72	7.48	7.29
	6-31G(d)	9.77	7.89	7.69	7.63	7.06
	6-311G(d,p)	9.69	7.78	7.61	7.59	6.93
	6-311G(d,p) (water phase)	13.32	10.83	10.42	10.60	9.62
HOMO	3-21	− 0.2726	− 0.2773	− 0.2779	− 0.2760	− 0.2781
	6-31G(d)	− 0.2809	− 0.2842	− 0.2846	− 0.2839	− 0.2855
	6-311G(d,p)	− 0.2847	− 0.2882	− 0.2883	− 0.2875	− 0.2893
	6-311G(d,p) (water phase)	− 0.2868	− 0.2871	− 0.2878	− 0.2872	− 0.2879
LUMO	3-21	0.1012	0.0975	0.0975	0.0983	0.0972
	6-31G(d)	0.0994	0.0964	0.0964	0.0967	0.0955
	6-311G(d,p)	0.0914	0.0882	0.0885	0.0888	0.0875
	6-311G(d,p) (water phase)	0.0866	0.0866	0.0861	0.0864	0.0860
ΔE	3-21	0.3738	0.3748	0.3754	0.3743	0.3753
	6-31G(d)	0.3808	0.3806	0.3810	0.3806	0.3810
	6-311G(d,p)	0.3761	0.3764	0.3768	0.3763	0.3768
	6-311G(d,p) (water phase)	0.3734	0.3737	0.3739	0.3736	0.3739

Table 3. Computed net Mulliken charge on the heteroatoms of the five molecules at the equilibrium ground state by the DFT (B3LYP) method.

Atoms	**1** (Lead compound)			**2** (Trifluoro)			**3** (Thiazole)			**4** (Pyrazine)			**5** (Benzoxazole)		
Basis set	3-21	6-31G(d)	6-311 G(d,p)	3-21	6-31G(d)	6-311 G(d,p)	3-21	6-31G(d)	6-311 G(d,p)	3-21	6-31G(d)	6-311 G(d,p)	3-21	6-31G(d)	6-311 G(d,p)
N(17)	−0.8304	−0.8036	−0.4843	−0.8281	−0.8040	−0.4854	−0.8273	−0.8044	−0.4864	−0.8291	−0.8038	−0.4848	−0.8276	−0.8043	−0.4860
O(20)	−0.4989	−0.5013	−0.3163	−0.4980	−0.5004	−0.3153	−0.4980	−0.5005	−0.3156	−0.4982	−0.5005	−0.3155	−0.4979	−0.5002	−0.3152
O(22)	−0.4762	−0.4525	−0.3054	−0.4753	−0.4518	−0.3046	−0.4754	−0.4519	−0.3047	−0.4755	−0.4518	−0.3047	−0.4753	−0.4516	−0.3045
O(23)	−0.5818	−0.6176	−0.3750	−0.5816	−0.6172	−0.3746	−0.5816	−0.6171	−0.3746	−0.5817	−0.6172	−0.3746	−0.5815	−0.6170	−0.3744
N(25)	−0.8337	−0.5190	−0.4886	−0.8341	−0.5194	−0.4889	−0.8340	−0.5196	−0.4891	−0.8340	−0.5195	−0.4890	−0.8341	−0.5197	−0.4891
N(37)	−0.6280	−0.5286	−0.4806	−0.6290	−0.5291	−0.4820	−0.6268	−0.5290	−0.4812	−0.6279	−0.5287	−0.4809	−0.6264	−0.5307	−0.4834
N(38)	−0.6855	−0.4932	−0.4697	−0.6842	−0.5068	−0.4761	−0.6523	−0.4513	−0.4291	−0.6919	−0.4993	−0.4697	−0.7230	−0.5283	−0.4870
N(48)	−0.6193	−0.5121	−0.3740	–	–	–	–	–	–	−0.5022	−0.3814	−0.2568	–	–	–
N(45)	–	–	–	–	–	–	−0.5598	−0.4711	−0.3474	–	–	–	–	–	–
S(46)	–	–	–	–	–	–	−0.4254	−0.1982	−0.2066	–	–	–	–	–	–
N(46)	–	–	–	–	–	–	–	–	–	−0.5872	−0.4904	−0.3374	–	–	–
F(50)	–	–	–	−0.2771	−0.2708	−0.2116	–	–	–	–	–	–	–	–	–
F(51)	–	–	–	−0.2707	−0.2624	−0.2111	–	–	–	–	–	–	–	–	–
F(52)	–	–	–	−0.2783	−0.2715	−0.2145	–	–	–	–	–	–	–	–	–
N(43)	–	–	–	–	–	–	–	–	–	–	–	–	−0.6272	−0.5841	−0.3928
O(52)	–	–	–	–	–	–	–	–	–	–	–	–	−0.5566	−0.5420	−0.3279

These heteroatoms are assumed to play the key role for anti-viral potency because these are the most negative centres of the molecules. So far as is known, the free radical centres of high electron densities capture the viruses through chemical attack.

HOMO and LUMO structures of the molecules are shown in Figures 3(a)–(e) and 4(a)–(e) and Figures 5(a)–(e) and 6(a)–(e), respectively, in the 6-311G(d,p) calculations by the DFT and HF methods. It was confirmed experimentally [7] that high antiviral activity was ensured by the region around the 4-keto-3-carboxylic moiety. The HOMO and LUMO structures support this. The concentrations of electron densities in the 4-keto-3-carboxylic moiety region in the HOMO of the five molecules are determined by both the methods. The electron densities are somewhat greater for the new potent molecules **2**–**5** that increase their high antiviral activity, which is in excellent agreement with the experimental findings [7]. The concentration of charges in the LUMO of all the molecules shows the same trend by both the methods except for molecule **4** by the DFT method. Here, the substituted pyrazine ring shows the substantial concentration of charges. This is a strange result by the DFT calculations, which may indicate that, in this molecule, the antiviral activity is expected to take place both in the 4-keto-3-carboxylic moiety and substituted pyrazine ring. The HF calculations are very reliable in this regard showing no such strange findings. The single-point water-phase calculations at the HF 6-311G(d,p) optimised geometries for all the molecules show that the charge densities have been more concentrated in the HOMO–LUMO structures (shown in Figures 7(a)–(e) and 8(a)–(e), respectively) than the gas phase that correlates very well with the drug action of the studied molecules, which is in excellent agreement with the experimental findings.

Tables 5 and 6 show some selected geometrical parameters of all the molecules by the DFT and HF methods, respectively. Some of the regions containing heteroatoms of different molecules (except F) are selected. From Tables 5 and 6, it can be seen that the 4-keto-3-carboxylic moiety part is planar for all the molecules in all calculations by both the methods irrespective of the substituents of the lead compound **1**. The (C_{28}—N_{38}—C_{39})/(C_{28}—N_{38}—C_{43})/(C_{28}—N_{38}—C_{42}) angles show sp^2 hybridisation of the N-atom in **1**, **2**, **4**, in **3** and in **5**, respectively, the variations being within ±5°. The (C_{27}—N_{37}—C_{11}) angle varies from 113.3 to 114.5° for all the molecules in all calculations. The (C_8—C_{11}—N_{37}), (C_1—N_{25}—C_{13}) and (C_9—C_{10}—N_{17}) angles also show very little variation of the sp^2 hybridisation of C- and N-atoms (119.60–123.7°). The distance N_{38}—C_{39}/N_{38}—C_{43}/N_{38}—C_{42} is in the range 1.37–1.41 Å for **1**, **2**, **4**, 1.34–1.36 Å for **5** and 1.35–1.37 Å for **3**, respectively. For the other C—N distances, the variation is from 1.37 to 1.47 Å for all the molecules in all calculations. The O—H distance varies from 0.96

Table 4. Computed net Mulliken charge on the heteroatoms of the five molecules at the equilibrium ground state by the HF method.

Basis set	3-21	6-31G(d)	6-311G(d,p)	6-311G(d,p) (water phase)	3-21	6-31G(d)	6-311G(d,p)	6-311G(d,p) (water phase)
Atoms	**1** (Lead compound)				**2** (Trifluoro)			
N(17)	−0.9852	−0.8967	−0.5589	−0.5920	−0.9808	−0.8966	−0.5594	−0.5913
O(20)	−0.6191	−0.5734	−0.4325	−0.5231	−0.6183	−0.5728	−0.4317	−0.5229
O(22)	−0.6029	−0.5424	−0.4241	−0.5079	−0.6021	−0.5419	−0.4236	−0.5078
O(23)	−0.7488	−0.7519	−0.4678	−0.4847	−0.7487	−0.7517	−0.4675	−0.4843
N(25)	−1.0858	−0.7688	−0.6631	−0.6588	−1.0864	−0.7693	−0.6636	−0.6591
N(37)	−0.8122	−0.7066	−0.6314	−0.6278	−0.8133	−0.7103	−0.6377	−0.6330
N(38)	−0.9290	−0.7190	−0.6222	−0.6267	−0.8431	−0.6884	−0.6130	−0.6222
N(48)	−0.7963	−0.6311	−0.4985	−0.5304	–	–	–	–
F(50)	–	–	–	–	−0.3924	−0.3683	−0.2870	−0.2963
F(51)	–	–	–	–	−0.3841	−0.3640	−0.2868	−0.2968
F(52)	–	–	–	–	−0.3929	−0.3692	−0.2945	−0.2996
	3 (Thiazole)				**4** (Pyrazine)			
N(17)	−0.9767	−0.8972	−0.5607	−0.5922	−0.9828	−0.8967	−0.5593	−0.5920
O(20)	−0.6183	−0.5728	−0.4318	−0.5227	−0.6184	−0.5727	−0.4317	−0.5227
O(22)	−0.6020	−0.5418	−0.4236	−0.5076	−0.6023	−0.5418	−0.4236	−0.5078
O(23)	−0.7487	−0.7516	−0.4674	−0.4845	−0.7487	−0.7517	−0.4675	−0.4845
N(25)	−0.0866	−0.7695	−0.6637	−0.6594	−1.0862	−0.7693	−0.6636	−0.6591
N(37)	−0.8126	−0.7072	−0.6336	−0.6304	−0.8126	−0.7063	−0.6311	−0.6278
N(38)	−0.8901	−0.6826	−0.5933	−0.5972	−0.9346	−0.7221	−0.6234	−0.6292
N(48)	–	–	–	–	−0.6079	−0.4509	−0.3197	−0.3701
N(45)	–	–	–	−0.5112	–	–	–	–
S(46)	–	–	–	0.2058	–	–	–	–
N(46)	–	–	–	–	−0.7476	−0.5867	−0.4355	−0.4612
	5 (Benzoxazole)							
N(17)	−0.9775	−0.8969	−0.5603	−0.5921				
O(20)	−0.6182	−0.5725	−0.4315	−0.5225				
O(22)	−0.6020	−0.5416	−0.4234	−0.5076				
O(23)	−0.7487	−0.7516	−0.4674	−0.4845				
N(25)	−1.0866	−0.7696	−0.6638	−0.6594				
N(37)	−0.8122	−0.7086	−0.6360	−0.6330				
N(38)	−0.9758	−0.7734	−0.6551	−0.6562				
N(43)	−0.7703	−0.6667	−0.5205	−0.5651				
O(52)	−0.7385	−0.6806	−0.4308	−0.4303				

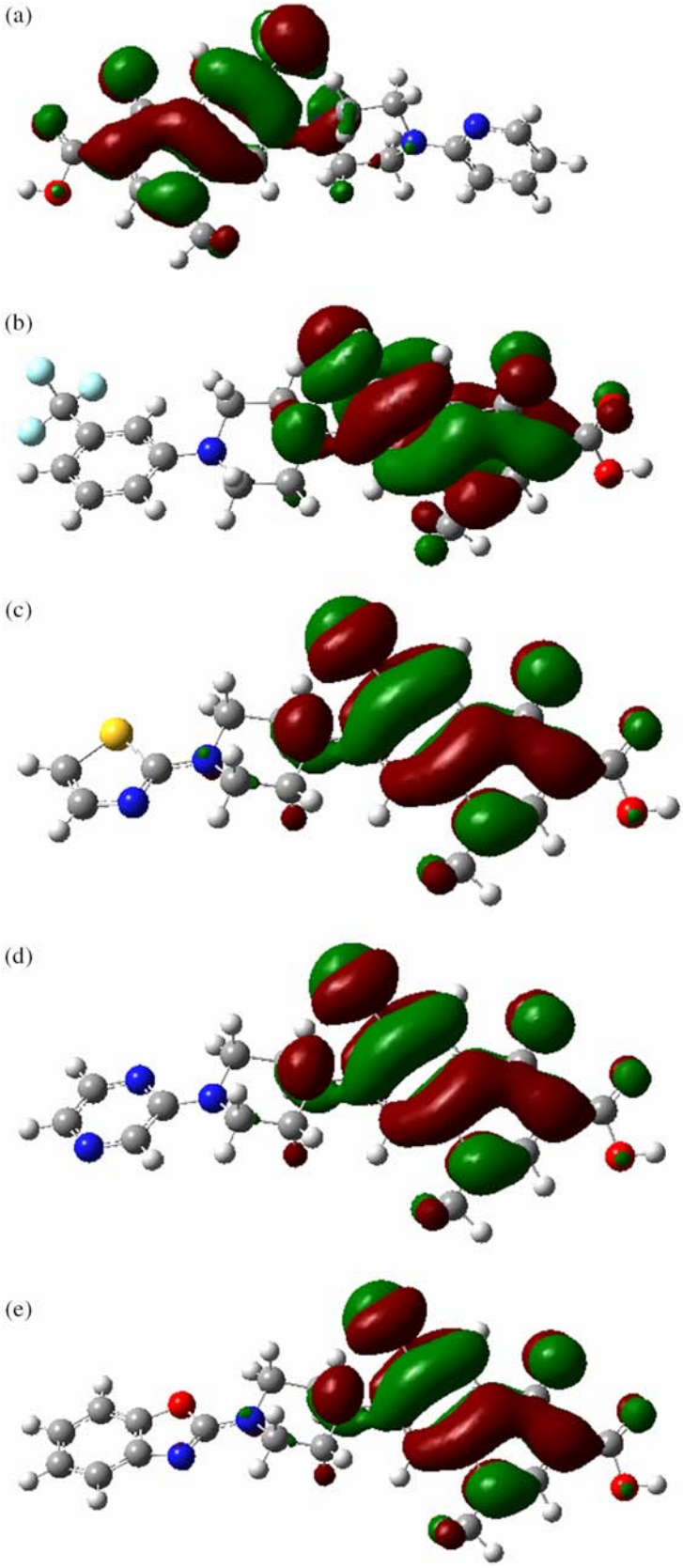

Figure 3. (a)–(e) HOMO structures of the five molecules (**1**–**5**), respectively, by the DFT (B3LYP) method (6-311G(d,p)).

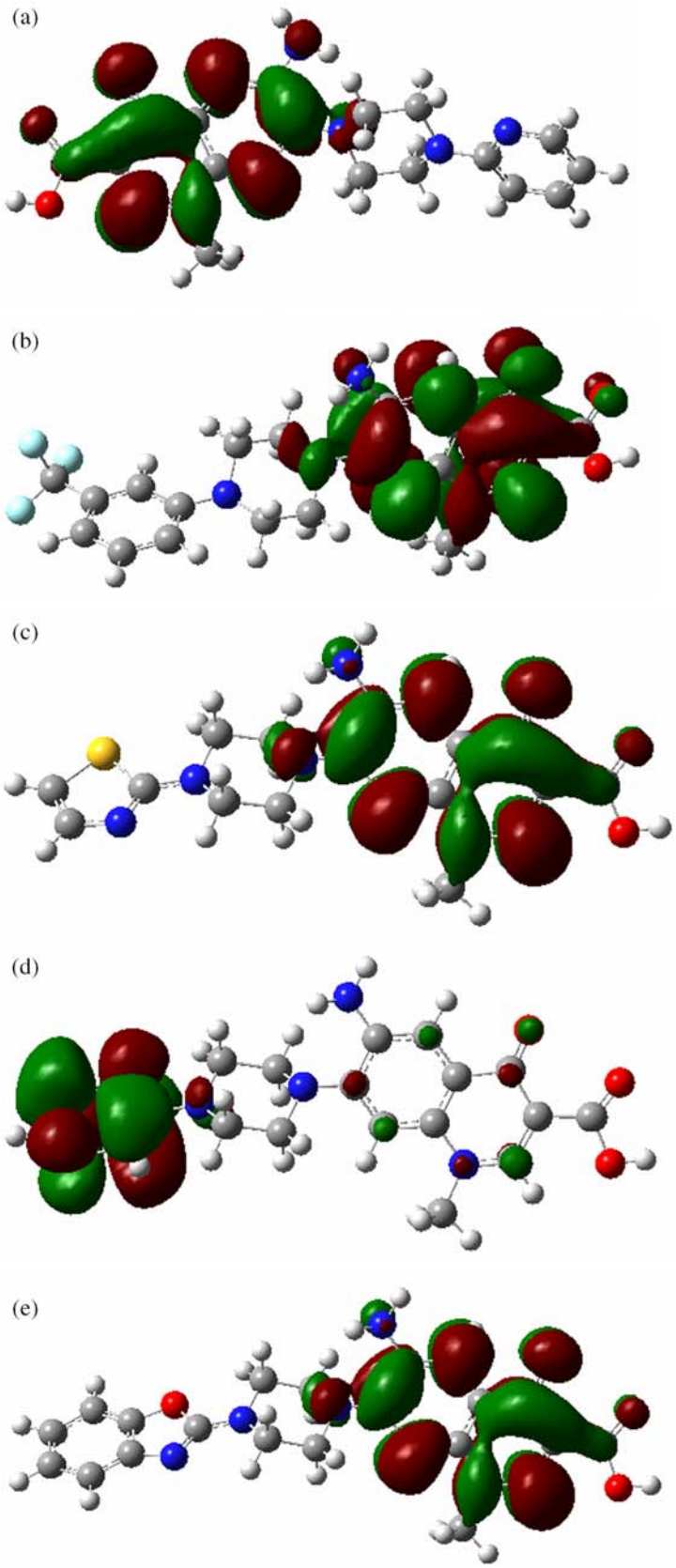

Figure 4. (a)–(e) LUMO structures of the five molecules (**1**–**5**), respectively, by the DFT (B3LYP) method (6-311G(d,p)).

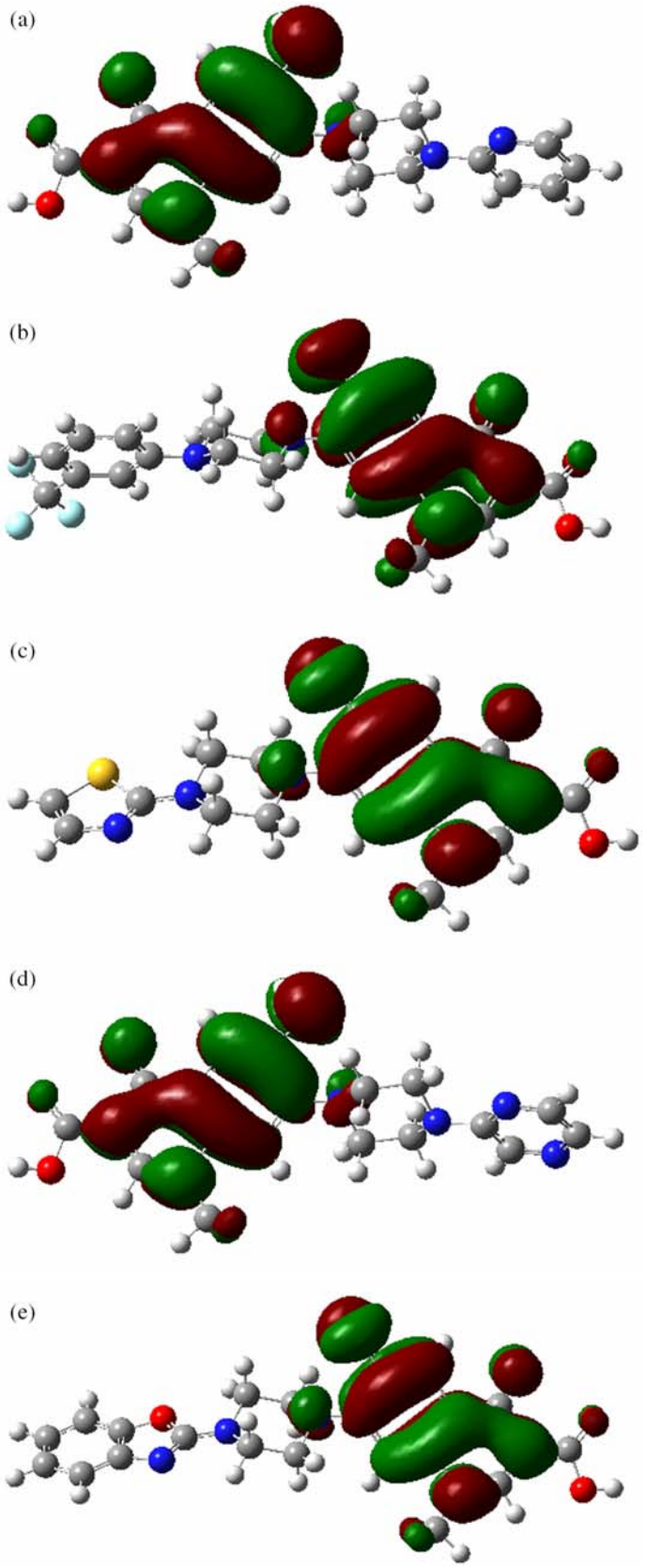

Figure 5. (a)–(e) HOMO structures of the five molecules (**1**–**5**), respectively, by the HF method (6-311G(d,p)).

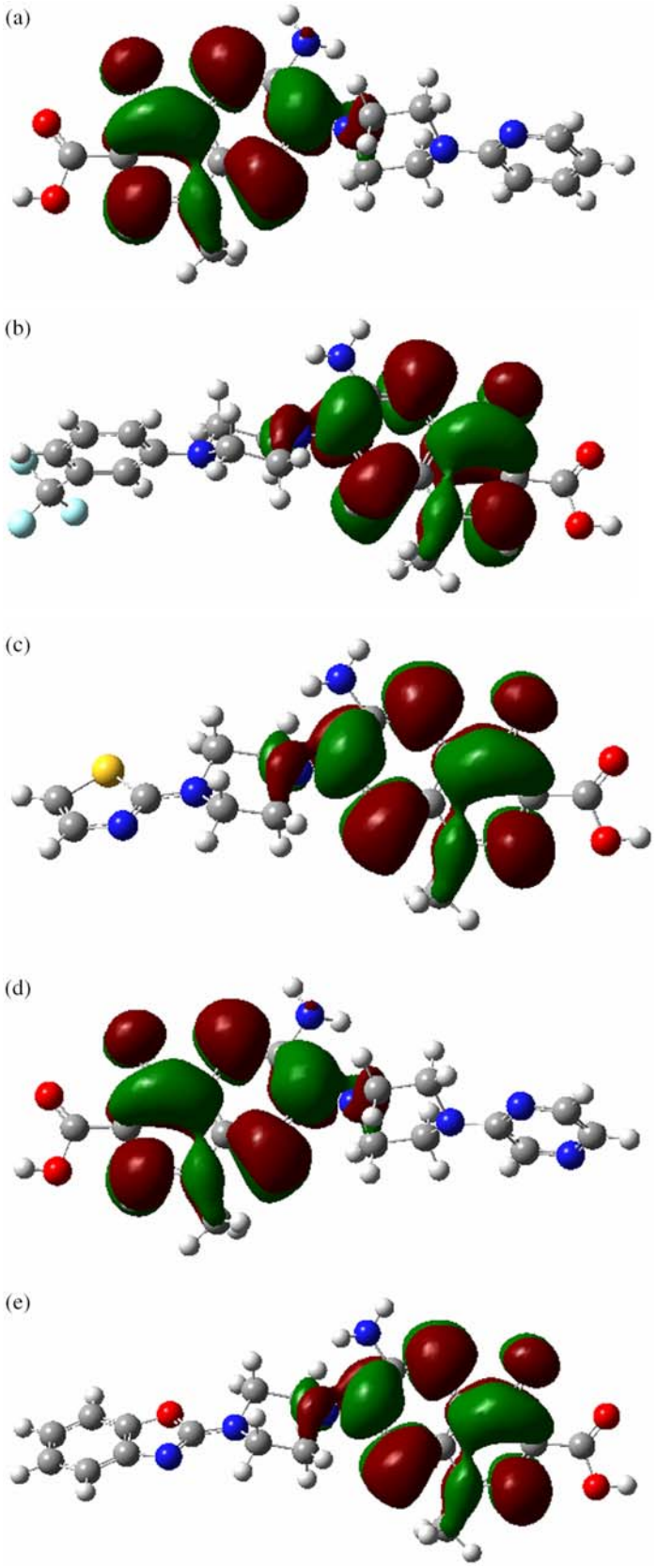

Figure 6. (a)–(e) LUMO structures of the five molecules (**1**–**5**), respectively, by the HF method (6-311G(d,p)).

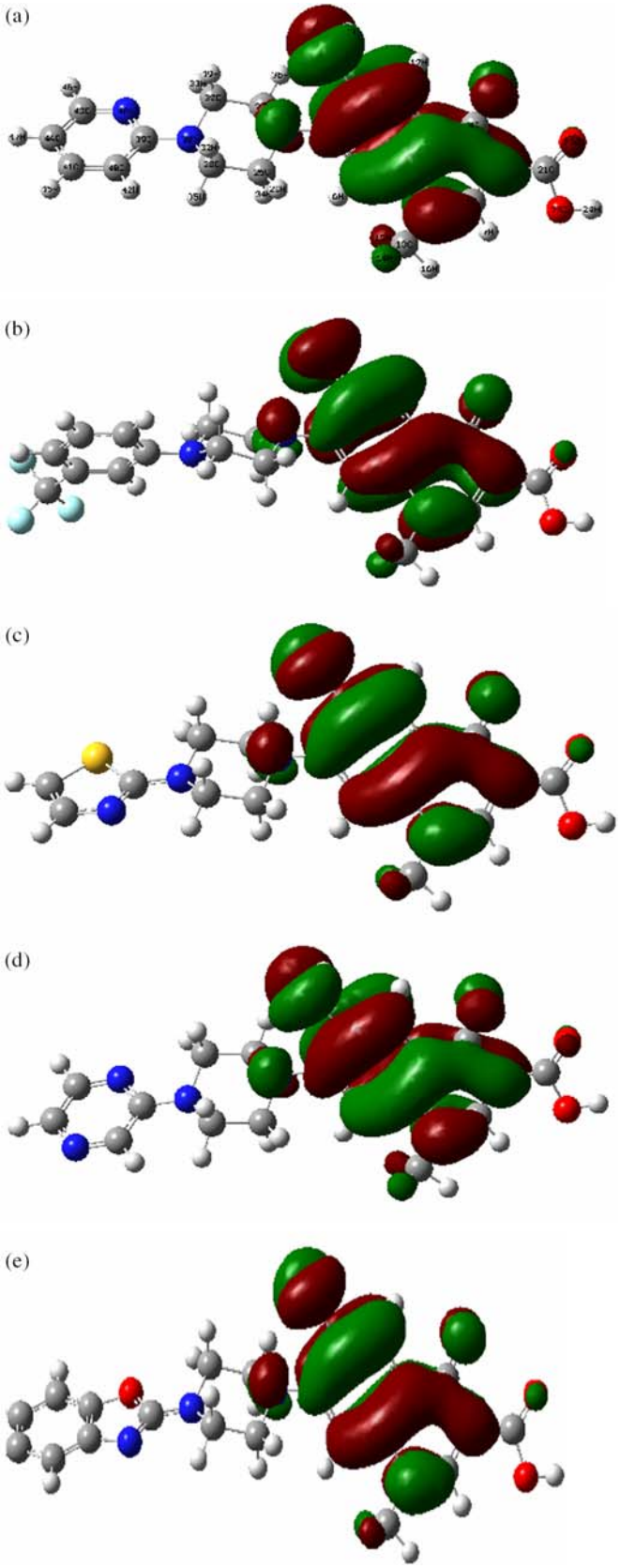

Figure 7. (a)–(e) HOMO structures of the five molecules (**1**–**5**), respectively, by the HF method (6-311G(d,p)) in the water phase.

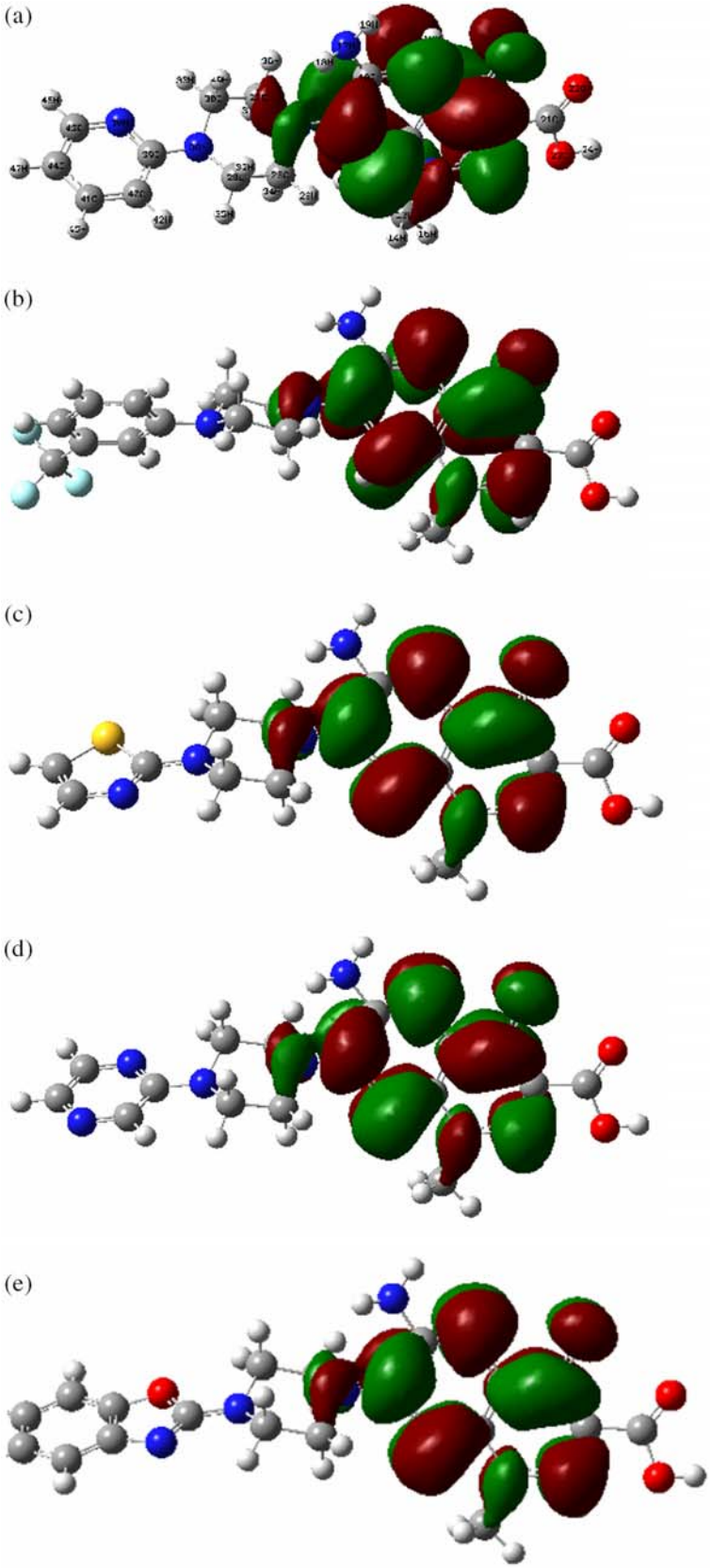

Figure 8. (a)–(e) LUMO structures of the five molecules (**1**–**5**), respectively, by the HF method (6-311G(d,p)) in the water phase.

Table 5. Computed values of some selected geometrical parameters (length in Å and angle in degree) in the equilibrium ground state of the five molecules by the DFT (B3LYP) method.

Molecules	Basis set	**1** (Lead compound)	**2** (Trifluoro)	**3** (Thiazole)	**4** (Pyrazine)	**5** (Benzoxazole)
$r(C_4—O_{20})$	3-21	1.2475	1.2474	1.2473	1.2474	1.2474
	6-31G(d)	1.2286	1.2284	1.2284	1.2284	1.2284
	6-311G(d,p)	1.2222	1.2220	1.2220	1.2220	1.2220
$r(C_5—C_{21})$	3-21	1.4630	1.4635	1.4634	1.4633	1.4635
	6-31G(d)	1.4759	1.4763	1.4762	1.4762	1.4763
	6-311G(d,p)	1.4763	1.4768	1.4767	1.4766	1.4768
$r(C_{21}—O_{22})$	3-21	1.2250	1.2249	1.2249	1.2249	1.2248
	6-31G(d)	1.2108	1.2107	1.2107	1.2107	1.2107
	6-311G(d,p)	1.2032	1.2031	1.2030	1.2031	1.2030
$r(C_{21}—O_{23})$	3-21	1.4080	1.4079	1.4079	1.4081	1.4078
	6-31G(d)	1.3783	1.3779	1.3778	1.3779	1.3778
	6-311G(d,p)	1.3778	1.3774	1.3775	1.3775	1.3773
$r(O_{23}—H_{24})$	3-21	0.9950	0.9950	0.9950	0.9950	0.9950
	6-31G(d)	0.9743	0.9743	0.9743	0.9743	0.9743
	6-311G(d,p)	0.9671	0.9672	0.9672	0.9672	0.9672
$r(C_{13}—N_{25})$	3-21	1.4773	1.4773	1.4776	1.4774	1.4776
	6-31G(d)	1.4597	1.4598	1.4600	1.4598	1.4600
	6-311G(d,p)	1.4605	1.4607	1.4608	1.4606	1.4608
$r(C_{10}—N_{17})$	3-21	1.3780	1.3802	1.3806	1.3792	1.3804
	6-31G(d)	1.3964	1.3972	1.3978	1.3968	1.3976
	6-311G(d,p)	1.3938	1.3946	1.3951	1.3943	1.3953
$r(C_{11}—N_{37})$	3-21	1.4340	1.4343	1.4357	1.4348	1.4359
	6-31G(d)	1.4231	1.4241	1.4243	1.4241	1.4249
	6-311G(d,p)	1.4217	1.4229	1.4229	1.4226	1.4236
$r(N_{38}—C_{39})$	3-21	1.3823	1.4024	1.3559**	1.3729	1.3452*
$r*(N_{38}—C_{42})$	6-31G(d)	1.3936	1.4103	1.3758**	1.3861	1.3607*
$r**(N_{38}—C_{43})$	6-311G(d,p)	1.3903	1.4073	1.3729**	1.3833	1.3566*
$\angle(C_8—C_{11}—N_{37})$	3-21	123.40	123.29	123.30	123.35	123.27
	6-31G(d)	122.98	122.87	122.88	122.96	122.89
	6-311G(d,p)	122.96	122.85	122.86	122.94	122.87
$\angle(C_1—N_{25}—C_{13})$	3-21	120.00	120.00	120.00	119.99	120.02
	6-31G(d)	119.80	119.81	119.80	119.80	119.82
	6-311G(d,p)	119.66	119.66	119.66	119.66	119.68
$\angle(C_9—C_{10}—N_{17})$	3-21	123.78	123.71	123.75	123.72	123.74
	6-31G(d)	122.13	122.15	122.15	122.13	122.15
	6-311G(d,p)	122.14	122.16	122.16	122.13	122.15
$\angle(C_{27}—N_{37}—C_{11})$	3-21	113.85	113.99	113.35	113.73	113.34
	6-31G(d)	114.54	114.42	114.09	114.40	113.98
	6-311G(d,p)	114.50	114.41	114.05	114.38	113.94
$\angle(C_{28}—N_{38}—C_{39})$	3-21	125.31	120.79	119.78*	125.11	120.03**
$\angle*(C_{28}—N_{38}—C_{43})$	6-31G(d)	121.06	118.21	116.94*	121.29	117.78**
$\angle**(C_{28}—N_{38}—C_{42})$	6-311G(d,p)	121.39	118.37	117.25*	121.54	118.22**
$\angle(C_4—C_5—C_{21}—O_{22})$	3-21	0.25	−0.10	0.27	0.21	−0.09
	6-31G(d)	0.20	0.07	0.05	0.14	0.15
	6-311G(d,p)	0.21	0.12	0.03	0.16	0.199
$\angle(C_5—C_{21}—O_{23}—H_{24})$	3-21	179.99	179.92	179.97	179.99	179.95
	6-31G(d)	179.99	179.96	179.99	179.99	179.99
	6-311G(d,p)	179.99	179.96	179.99	179.99	180.00

Note: * and ** signify the specific bond distances and angles in different molecules.

Table 6. Computed values of some selected geometrical parameters (length in Å and angle in degree) in the equilibrium ground state of the five molecules by the HF method.

Molecules	Basis set	**1** (Lead compound)	**2** (Trifluoro)	**3** (Thiazole)	**4** (Pyrazine)	**5** (Benzoxazole)
$r(C_4—O_{20})$	3-21	1.2211	1.2210	1.2210	1.2210	1.2210
	6-31G(d)	1.1995	1.1994	1.1994	1.1994	1.1994
	6-311G(d,p)	1.1939	1.1938	1.1938	1.1938	1.1937
$r(C_5—C_{21})$	3-21	1.4568	1.4572	1.4572	1.4571	1.4572
	6-31G(d)	1.4762	1.4763	1.4763	1.4763	1.4764
	6-311G(d,p)	1.4769	1.4771	1.4772	1.4771	1.4772
$r(C_{21}—O_{22})$	3-21	1.2017	1.2016	1.2016	1.2016	1.2016
	6-31G(d)	1.1856	1.1855	1.1855	1.1855	1.1855
	6-311G(d,p)	1.1793	1.1792	1.1792	1.1793	1.1792
$r(C_{21}—O_{23})$	3-21	1.3794	1.3789	1.3789	1.3791	1.3789
	6-31G(d)	1.3478	1.3476	1.3476	1.3476	1.3474
	6-311G(d,p)	1.3465	1.3463	1.3462	1.3463	1.3462
$r(O_{23}—H_{24})$	3-21	0.9671	0.9671	0.9671	0.9671	0.9671
	6-31G(d)	0.9515	0.9516	0.9516	0.9516	0.9516
	6-311G(d,p)	0.9447	0.9447	0.9447	0.9447	0.9447
$r(C_{13}—N_{25})$	3-21	1.4687	1.4689	1.4691	1.4688	1.4691
	6-31G(d)	1.4531	1.4532	1.4533	1.4531	1.4533
	6-311G(d,p)	1.4532	1.4533	1.4535	1.4533	1.4535
$r(C_{10}—N_{17})$	3-21	1.3771	1.3791	1.3808	1.3781	1.3804
	6-31G(d)	1.3972	1.3979	1.3985	1.3976	1.3985
	6-311G(d,p)	1.3969	1.3977	1.3983	1.3974	1.3983
$r(C_{11}—N_{37})$	3-21	1.4275	1.4275	1.4278	1.4278	1.4280
	6-31G(d)	1.4187	1.4193	1.4195	1.4193	1.4198
	6-311G(d,p)	1.4187	1.4194	1.4194	1.4192	1.4199
$r(N_{38}—C_{39})$	3-21	1.3714	1.4127	1.3420**	1.3642	1.3311*
$r*(N_{38}—C_{42})$	6-31G(d)	1.3889	1.4147	1.3686**	1.3855	1.3524*
$r**(N_{38}—C_{43})$	6-311G(d,p)	1.3872	1.4132	1.3676**	1.3847	1.3509*
$\angle(C_8—C_{11}—N_{37})$	3-21	122.76	122.69	122.67	122.72	122.67
	6-31G(d)	122.82	122.72	122.73	122.79	122.72
	6-311G(d,p)	122.81	122.70	122.72	122.78	122.70
$\angle(C_1—N_{25}—C_{13})$	3-21	120.21	120.20	120.19	120.20	120.19
	6-31G(d)	119.94	119.94	119.94	119.93	119.93
	6-311G(d,p)	119.82	119.83	119.83	119.82	119.83
$\angle(C_9—C_{10}—N_{17})$	3-21	123.03	123.01	122.99	123.00	122.99
	6-31G(d)	121.84	121.84	121.89	121.85	121.88
	6-311G(d,p)	121.85	121.84	121.88	121.86	121.87
$\angle(C_{27}—N_{37}—C_{11})$	3-21	114.19	114.20	113.86	114.16	113.84
	6-31G(d)	114.16	113.94	113.81	114.12	113.76
	6-311G(d,p)	114.00	113.78	113.65	113.95	113.60
$\angle(C_{28}—N_{38}—C_{39})$	3-21	125.38	119.03	119.92*	125.20	120.50**
$\angle*(C_{28}—N_{38}—C_{43})$	6-31G(d)	119.70	117.23	116.42*	119.51	117.23**
$\angle**(C_{28}—N_{38}—C_{42})$	6-311G(d,p)	119.72	117.24	116.52*	119.48	117.31**
$\angle(C_4—C_5—C_{21}—O_{22})$	3-21	0.10	0.09	0.06	0.09	0.06
	6-31G(d)	0.20	0.20	0.06	0.13	0.08
	6-311G(d,p)	0.19	0.17	0.05	0.17	0.08
$\angle(C_5—C_{21}—O_{23}—H_{24})$	3-21	179.94	179.94	179.98	179.96	179.98
	6-31G(d)	179.95	179.96	179.97	−179.95	179.98
	6-311G(d,p)	179.96	179.95	179.97	179.97	179.98

Note: * and ** signify the specific bond distances and angles in different molecules.

to 0.99 Å for all the molecules in all calculations. The C═O distance is within 1.20–1.24 Å and the other C—O distance is within 1.37–1.40 Å for all the molecules in all calculations. The calculated geometrical parameters are within the experimental range as expected.

4. Conclusion

The present study correlates very well with the experimental findings [7]. Compound **2** (trifluoro), **3** (thiazole), **4** (pyrazine) and **5** (benzoxazole) have been confirmed to be more effective than **1** (lead compound). The drug action in the water phase is also correlated by the presence of more electron-rich HOMO–LUMO structures. Almost similar conclusions are obtained in the present study for all the basis sets. In the present series, the HF calculations are more reliable.

References

[1] M. Baba, M. Okamoto, M. Makino, Y. Kimure, T. Ikeuchi, T. Sakaguchi, and T. Okamoto, *Potent and selective inhibition of human immunodeficiency virus type 1 transcription by piperazinyloxoquinoline derivatives*, Antimicrob. Agents Chemother. 41 (1997), pp. 1250–1255.

[2] M. Witvrouv, D. Daelemans, C. Pannecouque, J. Neyts, G. Anderi, R. Snoeck, A. Vandamme, J. Balzarini, J. Desmyter, M. Baba, and E. De Clercq, *Broad-spectrum antiviral activity of the piperazinylquinolone derivative K-12 and its mechanism of action*, Antiviral Chem. Chemother. 9 (1998), pp. 403–411.

[3] M. Baba, M. Okamoto, M. Kawamure, M. Makino, M. Higashida, T. Takashi, Y. Kimure, T. Ikeuchi, T. Tetsuka, and T. Okamoto, *Inhibition of human immunodeficiency virus type 1 replication and cytokine production by fluoroquinoline derivatives*, Mol. Pharmacol. 53 (1998), pp. 1097–1103.

[4] T. Ohmine, T. Katsube, Y. Tsuzaki, M. Kazui, N. Kobayashi, T. Komai, M. Hagihara, T. Nishigaki, A. Iwamoto, T. Kimure, H. Kashiwase, and M. Yamashita, *Anti-HIV-1 activities and pharmacokinetics of new arylpiperazinyl fluoroquinolones*, Bioorg. Med. Chem. Lett. 12 (2002), pp. 739–742.

[5] M. Hagihara, H. Kashiwase, T. Katsube, T. Komai, K. Momota, T. Ohmine, T. Nishigaki, S. Kimure, and K. Shimada, *Synthesis and anti-HIV activity of arylpiperazinyl fluoroquinolones: A new class of anti-HIV agents*, Bioorg. Med. Chem. Lett. 9 (1999), pp. 3063–3068.

[6] V. Cecchetti, C. Parolin, S. Moro, T. Pecere, E. Filipponi, A. Calistri, O. Tabarrini, B. Gatto, M. Palumbo, A. Fravolini, and G. Palu, *6-Aminoquinolones as new potential anti-HIV agents*, J. Med. Chem. 43 (2000), pp. 3799–3802.

[7] O. Tabarrini, M. Stevens, V. Cecchetti, S. Sabatini, M. Dell'Uomo, G. Manfroni, M. Palumbo, C. Pannecouque, E. De Clercq, and A. Fravolini, *Structure modifications of 6-aminoquinolones with potent anti-HIV activity*, J. Med. Chem. 47 (2004), pp. 5567–5578.

[8] M.J. Frisch, G.W. Trucks, H.B. Schlegel, G.E. Scuseria, M.A. Robb, J.R. Cheeseman, J.A. Montgomery, T. Vreven, Jr., K.N. Kudin, J.C. Burant, J.M. Millam, S.S. Iyengar, J. Tomasi, V. Barone, B. Mennucci, M. Cossi, G. Scalmani, N. Rega, G.A. Petersson, H. Nakatsuji, M. Hada, M. Ehara, K. Toyota, R. Fukuda, J. Hasegawa, M. Ishida, T. Nakajima, Y. Honda, O. Kitao, H. Nakai, M. Klene, X. Li, J.E. Knox, H.P. Hratchian, J.B. Cross, C. Adamo, J. Jaramillo, R. Gomperts, R.E. Stratmann, O. Yazyev, A.J. Austin, R. Cammi, C. Pomelli, J.W. Ochterski, P.Y. Ayala, K. Morokuma, G.A. Voth, P. Salvador, J.J. Dannenberg, V.G. Zakrzewski, S. Dapprich, A.D. Daniels, M.C. Strain, O. Farkas, D.K. Malick, A.D. Rabuck, K. Raghavachari, J.B. Foresman, J.V. Ortiz, Q. Cui, A.G. Baboul, S. Clifford, J. Cioslowski, B.B. Stefanov, G. Liu, A. Liashenko, P. Piskorz, I. Komaromi, R.L. Martin, D.J. Fox, T. Keith, M.A. Al-Laham, C.Y. Peng, A. Nanayakkara, M. Challacombe, P.M.W. Gill, B.G. Johnson, W. Chen, M.W. Wong, C. Gonzalez, and J.A. Pople, *Gaussian, Inc.*, Wallingford, CT, 2004.

[9] C. Lee, W. Yang, and R.G. Parr, *Development of the Colle–Salvetti correlation-energy formula into a functional of the electron density*, Phys. Rev. B 37 (1988), pp. 785–789.

[10] A.D. Becke, *Density-functional thermochemistry. III. The role of exact exchange*, J. Chem. Phys. 98 (1993), pp. 5648–5652.